Entropy production in high-energy heavy-ion collisions and the correlation of shear viscosity and thermalization time

A. Dumitru,[1] E. Molnár,[2] and Y. Nara[1,3]

[1]*Institut für Theoretische Physik, Johann Wolfgang Goethe Universität, Max-von-Laue-Str. 1, D-60438 Frankfurt am Main, Germany*

[2]*Frankfurt Institute for Advanced Studies, Johann Wolfgang Goethe Universität, Max-von-Laue-Str. 1, D-60438 Frankfurt am Main, Germany*

[3]*Akita International University 193-2 Okutsubakidai, Yuwa-Tsubakigawa, Akita 010-1211, Japan*

(Received 20 June 2007; published 23 August 2007)

We study entropy production in the early stage of high-energy heavy-ion collisions due to shear viscosity. We employ the second-order theory of Israel-Stewart with two different stress relaxation times, as appropriate for strong coupling or for a Boltzmann gas, respectively, and compare the hydrodynamic evolution. Based on the present knowledge of initial particle production, we argue that entropy production is tightly constrained. We derive new limits on the shear viscosity to entropy density ratio η/s, independent from elliptic flow effects, and determine the corresponding Reynolds number. Furthermore, we show that for a given entropy production bound, the initial time τ_0 for hydrodynamics is correlated to the viscosity. The conjectured lower bound for η/s provides a lower limit for τ_0.

DOI: 10.1103/PhysRevC.76.024910 PACS number(s): 25.75.−q, 12.38.Mh, 24.10.Nz

I. INTRODUCTION

Experiments conducted with colliding beams of gold ions at the BNL Relativistic Heavy-Ion Collider (RHIC) have confirmed that dense QCD matter exhibits hydrodynamic flow effects [1]. Their magnitude matches approximately predictions based on ideal Euler (inviscid) hydrodynamics[1] [2]. More precisely, the transverse momentum and centrality dependence of the azimuthally asymmetric flow, v_2, requires a shear viscosity to entropy density ratio as low as $\eta/s \leqslant 0.2$ [4–7]; this is much lower than perturbative extrapolations to temperatures $T \simeq 200$ MeV [8]. However, it is comparable to recent results for SU(3) pure gauge theory from the lattice [9] and to the conjectured lower bound for strongly coupled systems $\eta/s \geqslant 1/(4\pi)$ [10]. Similar constraints on η/s have been derived from transverse momentum correlations [11] and from energy loss and flow of heavy quarks at RHIC [12].

The purpose of this paper is to obtain an independent upper bound on η/s by analyzing entropy production in the early stages of the hydrodynamic evolution (the plasma phase), where the expansion rate and hence the entropy production rate is largest. Entropy production in heavy-ion collisions due to viscous effects has been studied before [13,14]. The new idea pursued here is that recent progress in our understanding of gluon production in the *initial* state constrains the amount of additional entropy produced via *final-state* interactions, and hence the viscosity and the thermalization time. The second-order formalism for viscous hydrodynamics of Israel and Stewart [15], and its application to one-dimensional boost-invariant Bjorken expansion [16], are briefly reviewed in Sec. II.

The initial condition for hydrodynamics, in particular the initial parton or entropy density in the central rapidity region, plays a crucial role. If it is close to the measured final-state multiplicity, this provides a stringent bound on viscous effects. The initial parton multiplicity in heavy-ion collisions cannot, of course, be measured directly. Our analysis therefore necessarily relies on a calculation of the initial conditions (presented in Sec. III). Specifically, we employ here a $k_\perp$-factorized form of the color glass condensate (CGC) approach which includes perturbative gluon saturation at small light-cone momentum fractions x [17]. However, different approaches for initial particle production, such as the HIJING model which relies on collinear factorization supplemented with an additional model for the soft regime, also predicts multiplicities close to experiment [18]. The same is true when the heavy-ion collision is modeled as a collision of two classical Yang-Mills fields [19]. It is important to test these models for small systems, such as peripheral $A + A$ (or even $p + p$) collisions, in order to constrain the entropy increase via final-state effects (thermalization and viscosity).

Section IV contains our main results. We show how the entropy production bound correlates η/s to the initial time for hydrodynamic evolution, τ_0. The entropy production rate grows with the expansion rate (i.e., how rapidly the flow lines diverge from each other), and the total amount of produced entropy is therefore rather sensitive to the early stages of the expansion. The bound on the viscosity depends also on the initial condition for the stress, which in the second-order theory is an independent variable and is not fixed by the viscosity and the shear [unless the stress relaxation time is extremely short, as predicted recently from the anti-de-Sitter space/conformal field theory (AdS/CFT) correspondence at strong coupling [20]].

In a recent paper, Lublinsky and Shuryak point out that if the initial time τ_0 is assumed to be very small, then a resummation of the viscous corrections to all orders in gradients of the velocity field is required [21]. Here, we explore only the regime where τ_0 is several times larger than the sound attenuation length Γ_s, and so the standard approach to viscous hydrodynamics should apply. Quantitatively, we

[1]Numerical solutions of Euler hydrodynamics on finite grids always involve some amount of numerical viscosity for stability. Reliable algorithms such as flux-corrected transport keep this numerical viscosity and the associated entropy production at a minimum [3].

find that an entropy bound of $\simeq$10% restricts η/s to be at most a *few* times the lower bound $[\eta/s = 1/(4\pi)]$ conjectured from the correspondence [10]. On the other hand, somewhat surprisingly, we find that even $\eta/s = 1/(4\pi)$ is large enough to give noticeable entropy production for thermalization times τ_0 well below 1 fm/c (but still larger than Γ_s). Present constraints from initial and final multiplicities are not easily reconciled with such extremely short initial times [22].

We restrict ourselves here to the 1+1D Bjorken expansion. Given its (numerical) simplicity and the fact that the entropy production rate is largest at early times, this should provide a reasonable starting point. Estimates for the initial time τ_0, for the parton density and the stress at τ_0, and for the viscosity to entropy density ratio η/s are in fact most welcome for large-scale numerical studies of relativistic (second-order) dissipative fluid dynamics. Without guidance on the initial conditions, the hydrodynamic theory can at best provide qualitative results for heavy-ion collisions.

We neglect any other possible source of entropy but shear viscosity at early times.[2] Even within this simplified setting, there could be additional entropy production due to a viscous "hadronic corona" surrounding the fireball [23], which we do not account for. Clearly, any additional contribution would further tighten the (upper) bound on η/s and the (lower) bound on τ_0. We also assume that η/s is constant. This does not hold over a very broad range of temperature [8] but should be a reasonable first approximation for $T \simeq 200$–400 MeV.

We employ natural units throughout the paper: $\hbar = c = k_B = 1$.

II. DISSIPATIVE FLUID DYNAMICS

A. Second-order formalism

In this section we briefly review some general expressions for viscous hydrodynamics which will be useful in the following discussion. More extensive discussions are given in Refs. [14,24–30], for example.

A single-component fluid is generally characterized by a conserved current (possibly more) N^μ, the energy-momentum tensor $T^{\mu\nu}$, and the entropy current S^μ. The conserved quantities satisfy the continuity equations

$$\partial_\mu N^\mu = 0, \quad \partial_\mu T^{\mu\nu} = 0. \tag{1}$$

In addition, the divergence of the entropy current has to be positive by the second law of thermodynamics, that is,

$$\partial_\mu S^\mu \geqslant 0. \tag{2}$$

For a perfect fluid, a well-defined initial-value problem requires the knowledge of $T^{\mu\nu}$ and N^μ on a spacelike surface in 3+1D Minkowski space time. This is equivalent to specifying the initial flow field u^μ, proper charge density $n \equiv u_\mu N^\mu$, and proper energy density $e \equiv u_\mu u_\nu T^{\mu\nu}$; the pressure is determined via an algebraic relation to e and n, the equation of state (EOS).

[2]This contribution is expected to vanish once transverse expansion is fully developed, see Sec. II B.

In dissipative fluids, irreversible viscous and heat conduction processes occur. These quantities can be expressed explicitly if the charge and entropy currents and the energy-momentum tensor are decomposed (projected) into their components parallel and perpendicular to the flow of matter [31]; the latter describe the dissipative currents. The transverse projector is given by $\Delta^{\mu\nu} = g^{\mu\nu} - u^\mu u^\nu$, with $g^{\mu\nu} = \mathrm{diag}(1, -1, -1, -1)$ the metric of flat space time. In the following, we focus on locally charge-neutral systems where all conserved currents vanish identically.

The energy-momentum tensor can be decomposed in the following way:

$$T^{\mu\nu} = eu^\mu u^\nu - (p + \Pi)\Delta^{\mu\nu} + W^\mu u^\nu + W^\nu u^\mu + \pi^{\mu\nu}. \tag{3}$$

Here, $W^\mu = q^\mu + hV^\mu = u_\nu T^{\nu\alpha}\Delta^\mu_\alpha$ is the energy flow, with $h = (e + p)/n$ the enthalpy per particle, q^μ is the heat flow, and $V^\mu = \Delta^{\mu\nu}N_\nu$ is the charge flow; we shall define the local rest-frame via $W^\mu = 0$ (the Landau frame). Furthermore, Π denotes the bulk pressure such that $p + \Pi = -\frac{1}{3}\Delta_{\mu\nu}T^{\mu\nu}$, while the symmetric and traceless part of the energy-momentum tensor defines the stress tensor, $\pi^{\mu\nu} = [\frac{1}{2}(\Delta^\mu_\alpha\Delta^\nu_\beta + \Delta^\nu_\alpha\Delta^\mu_\beta) - \frac{1}{3}\Delta^{\mu\nu}\Delta_{\alpha\beta}]T^{\alpha\beta}$.

The entropy current is decomposed as

$$S^\mu = su^\mu + \Phi^\mu. \tag{4}$$

In the standard first-order theory due to Eckart [31] and Landau and Lifshitz [32], only linear corrections are taken into account, i.e., $\Phi^\mu = q^\mu/T$. On the other hand, the second-order theory of relativistic dissipative fluid dynamics includes terms to second order in the irreversible flows and in the stress tensor [15], that is,

$$S^\mu = su^\mu + \frac{q^\mu}{T} - (\beta_0\Pi^2 - \beta_1 q_\nu q^\nu + \beta_2\pi_{\nu\alpha}\pi^{\nu\alpha})\frac{u^\mu}{2T} - \frac{\alpha_0\Pi q^\mu}{T} + \frac{\alpha_1\pi^{\mu\nu}q_\nu}{T}, \tag{5}$$

where the coefficients β_0, β_1, β_2 and α_0, α_1 represent thermodynamic integrals which (near equilibrium) are related to the relaxation times of the dissipative corrections. Furthermore, from Eq. (2), one can find linear relationships between the thermodynamic forces and fluxes, leading to the transport equations describing the evolution of dissipative flows [15].

In what follows, we will focus on shear effects and neglect heat flow and bulk viscosity; hence, Eq. (3) simplifies to

$$T^{\mu\nu} = eu^\mu u^\nu - p\Delta^{\mu\nu} + \pi^{\mu\nu}. \tag{6}$$

The stress tensor satisfies the relaxation equation

$$\tau_\pi u^\lambda\partial_\lambda\pi^{\mu\nu} + \pi^{\mu\nu} = 2\eta\sigma^{\mu\nu}, \tag{7}$$

where η denotes the shear viscosity, and the shear tensor $\sigma^{\mu\nu}$ is a purely "geometrical" quantity determined by the flow field as

$$\sigma^{\mu\nu} = \tfrac{1}{2}(\nabla^\mu u^\nu + \nabla^\nu u^\mu) - \tfrac{1}{3}\Delta^{\mu\nu}\nabla_\lambda u^\lambda, \tag{8}$$

with $\nabla^\mu = \Delta^{\mu\nu}\partial_\nu$. The relaxation time τ_π determines how rapidly the stress tensor $\pi^{\mu\nu}$ relaxes to the shear tensor $\sigma^{\mu\nu}$; in particular, in the limit $\tau_\pi \to 0$,

$$\pi^{\mu\nu} = 2\eta\sigma^{\mu\nu} \tag{9}$$

satisfies the same algebraic relation as in the first-order theory. The limit $\tau_\pi \to 0$ is formal, however, since the deviation of the stress $\pi^{\mu\nu}$ from $2\eta\sigma^{\mu\nu}$ at any given time, as obtained by solving Eq. (7), depends also on its initial value. If Eq. (9) is approximately valid at the initial time, then the first-order theory may provide a reasonable approximation for the entire evolution (see below).

By analyzing the correlation functions of the stress that lead to the definitions (7) and (9), respectively, of the shear viscosity, Koide argues that in the second-order theory of Israel and Stewart, η may represent a different quantity than in the first-order approach [33]. Nevertheless, here we assume that the conjectured lower bound for η/s applies even to the causal (second-order) approach.

B. Dissipative Bjorken scaling fluid dynamics

In this section we recall the 1+1D Bjorken scaling solution [16] in 3+1D space time including stress [14]. By assumption, the fluid in the central region of a heavy-ion collision expands along the longitudinal z direction only, with a flow velocity v equal to z/t. This is appropriate for times less than the transverse diameter R of the collision zone divided by the speed of sound $c_s = \sqrt{\partial p/\partial e}$ (possibly longer for very viscous fluids). After that, transverse expansion is fully developed, and we expect that entropy production due to shear decreases. In fact, it is straightforward to check that for *three-dimensional* scaling flow[3] $u_\mu \partial_\nu \sigma^{\mu\nu} = 0$; hence, within the first-order theory at least, the shear viscosity no longer enters into the evolution equation of the energy density.

Formulations of the Israel-Stewart second-order theory for Bjorken plus transverse expansion have been published [24–29] but require large-scale numerical computations. A relatively straightforward 1+1D analysis is warranted as a first step to provide an estimate for entropy production.

It is convenient to transform from (t, z) to new $(\tau, \tilde{\eta})$ coordinates, where $\tau = \sqrt{t^2 - z^2}$ denotes proper time and $\tilde{\eta} = \frac{1}{2}\log[(t+z)/(t-z)]$ is the space-time rapidity; for the Bjorken model, it is equal to the rapidity of the flow, $\eta_{\rm fl} \equiv \frac{1}{2}\log[(1+v)/(1-v)]$. In other words, the four-velocity of the fluid is $u^\mu = (\delta^{\mu 0} + \delta^{\mu 3})x^\mu/\tau$.

The longitudinal projection of the continuity equation for the stress-energy tensor then yields

$$\frac{de}{d\tau} + \frac{e+p}{\tau} - \frac{\Phi}{\tau} + \frac{\Pi}{\tau} = 0\,. \tag{10}$$

Here, e is the energy density of the fluid in the local rest frame, while p denotes the pressure. These quantities are related through the EOS. We focus here on entropy production during the early stages of evolution where the temperature is larger than the QCD cross-over temperature $T_c \simeq 170$ MeV, and so we assume a simple ideal-gas EOS, $p = e/3$.

In what follows, we will neglect the bulk pressure Π which would otherwise tend to increase entropy production further. Well above T_c, this contribution is expected to be much smaller than that due to shear [34]. In the transition region, the bulk viscosity could be significant [35]. Also, for the 1+1D expansion considered here, the stress $\Phi \equiv \pi^{00} - \pi^{zz}$ acts in the same way as the bulk pressure Π: only the combination $\Phi - \Pi$ appears in Eq. (10).

The time evolution of the stress is determined by [14]

$$\frac{d\Phi}{d\tau} + \frac{\Phi}{\tau_\pi} + \frac{\Phi}{2}\left[\frac{1}{\tau} + \frac{T}{\beta_2}\frac{d}{d\tau}\left(\frac{\beta_2}{T}\right)\right] - \frac{2}{3\beta_2\tau} = 0. \tag{11}$$

τ_π sets the time scale for relaxation to the *first-order* theory where $\Phi_{\text{1st-O}} = 4\eta/3\tau$ (*not* to the ideal-fluid limit $\Phi = 0$). It is related to η and β_2 via $\tau_\pi = 2\eta\beta_2$. For a classical Boltzmann gas of massless particles, $\beta_2 = 3/(4p) = 3/(Ts)$ and so

$$\tau_\pi = \frac{6}{T}\frac{\eta}{s}. \tag{12}$$

At infinite coupling, from the AdS/CFT correspondence, $\eta/s = 1/(4\pi)$ [10] and $\tau_\pi = (1 - \log 2)/(6\pi T)$ [20]. For large but finite coupling, we assume that $\eta\beta_2$ and thus τ_π are proportional to η/s, i.e., that $\beta_2 = (3r)/(Ts)$ with $r = (1 - \log 2)/9$; then

$$\tau_\pi = r\frac{6}{T}\frac{\eta}{s}. \tag{13}$$

Note that the numerical prefactor r is about 30 times smaller than for a Boltzmann gas, implying much faster relaxation of the dissipative fluxes to the first-order theory.

One can also define a Reynolds number via the ratio of nondissipative to dissipative quantities [36], $R = (e+p)/\Phi$. Equation (10) can then be written as

$$\frac{de}{d\log\tau} = (R^{-1} - 1)(e+p)\,, \tag{14}$$

where we have neglected the bulk pressure. For stability, the effective enthalpy $(e+p)(1-1/R)$ should be positive, i.e., $R > 1$. The energy density then decreases monotonically with time.

The equations of second-order dissipative fluid dynamics, Eqs. (10) or (14) and (11), together with Eqs. (12) or (13) and $\beta_2 = \tau_\pi/(2\eta)$ form a closed set of equations for a fluid with vanishing currents, if augmented by an EOS. Furthermore, the initial energy density $e_0 \equiv e(\tau_0)$ and the initial shear $\Phi_0 \equiv \Phi(\tau_0)$ have to be given. In the second-order theory, one has to specify the initial condition for the viscous stress Φ_0 independently from the initial energy or particle density. We are presently unable to compute Φ_0. Below, we shall therefore present results for various values of Φ_0.

Alternatively, a physically motivated initial value Φ_0^* for the stress can be obtained from the condition that $dR/d\tau = 0$ at $\tau = \tau_0$. This is the "tipping point" between a system that is already approaching perfect fluidity at τ_0 ($dR^{-1}/d\tau < 0$, if $\Phi_0 > \Phi_0^*$) and one that is unable to compete with the expansion and is in fact departing from equilibrium ($dR^{-1}/d\tau > 0$, if $\Phi_0 < \Phi_0^*$) for at least some time after τ_0.

For an EOS with constant speed of sound, say $p = e/3$, the condition that $\dot{R} = 0$ is equivalent to $\dot{e}/e = \dot{\Phi}/\Phi$.

[3] Replace $z \to |\boldsymbol{r}|$ in the definition of proper time τ and space-time rapidity $\tilde{\eta}$ below, and take $\boldsymbol{u} = \boldsymbol{r}/\tau$.

Equations (10) and (11) then yield

$$\frac{\Phi_0^*}{e_0} = \frac{4}{3}\frac{\tau_0}{\tau_\pi}\left[\sqrt{1+\frac{4}{9r}\frac{\tau_\pi^2}{\tau_0^2}}-1\right] \tag{15}$$

$$\approx \frac{8}{27r}\frac{\tau_\pi}{\tau_0} \quad \left(\tau_\pi/\tau_0 \ll \sqrt{r}\right), \tag{16}$$

$$= \frac{16}{9}\frac{1}{T_0\tau_0}\frac{\eta}{s} \text{ (first-order theory)}. \tag{17}$$

The second line applies in the limit of short relaxation time; since τ_π is proportional to r, this is always satisfied in the limit $r \to 0$. For typical initial conditions relevant to heavy-ion collisions, it is a reasonable approximation even in the Boltzmann limit ($r = 1$). In Eq. (17) we have indicated that Eq. (16) is in fact nothing but the stress in the first-order theory (divided by the initial energy density). While it is clear that Φ relaxes to $\Phi_{\text{1st-O}}$ over time scales on the order of τ_π, Eq. (17) is actually a statement about the *initial* value of Φ: in a fluid with reasonably short relaxation time and stationary initial Reynolds number, $\dot{R}(\tau_0) = 0$, even the initial value of the stress is given by the first-order approach.

The condition $R(\tau_0) > 1$ for applicability of hydrodynamics together with Eq. (16) then provides the following lower bound on τ_0:

$$\tau_0 > \frac{4}{3T_0}\frac{\eta}{s} \equiv \Gamma_s(\tau_0), \tag{18}$$

where Γ_s denotes the sound attenuation length; within the first-order approach, $R = \tau/\Gamma_s$. The factor of η/s on the right-hand side illustrates the extended range of applicability of hydrodynamics as compared to a Boltzmann equation: a classical Boltzmann description requires that the thermal de Broglie wave length, $\sim 1/T$, is smaller than the (longitudinal) size of the system, τ. For very small viscosity, though, hydrodynamics is applicable (since $R \gg 1$) even when $\Gamma_s \ll \tau \lesssim 1/T$. In this point we differ somewhat from Lublinsky and Shuryak [21], who argue that the theory needs to be resummed to all orders in the gradients of the velocity field already when $\tau \sim 1/T$. From our argument above, this should be necessary only when $\tau_0 \sim \Gamma_s(\tau_0)$, which is much smaller than $1/T_0$ if $\eta/s \ll 1$.

The purpose of this paper is to motivate, however, that a much stronger constraint than $\tau_0 > \Gamma_s(\tau_0)$ may result from a bound on entropy production (which follows from the centrality dependence of the multiplicity), cf. Sec. IV.

In the Bjorken model, the entropy per unit rapidity and transverse area at time τ is given by

$$\frac{1}{A_\perp}\frac{dS(\tau)}{d\eta} = \tau\tilde{s}(\tau), \tag{19}$$

where $A_\perp$ is the transverse area, while $\tilde{s} \equiv S^\mu u_\mu$ denotes the longitudinal projection of the entropy current. Neglecting heat flow ($q^\mu = 0$) and bulk pressure ($\Pi = 0$), one obtains from Eq. (5)

$$\tilde{s} = s\left(1 - \frac{3}{4}\frac{\beta_2}{Ts}\Phi^2\right). \tag{20}$$

$\tilde{s}$ can be determined, for any $\tau \geqslant \tau_0$, from the solution of Eqs. (10) and (11). Note that the second term in Eq. (20) is of order $(\Phi/e)^2$. For nearly perfect fluids with $\eta/s \ll 1$ and $\dot{R}(\tau_0) = 0$, it is rather small.

III. THE CGC INITIAL CONDITION

Before we can present solutions of the hydrodynamic equations, we need to determine suitable initial conditions. To date, the most successful description of the centrality dependence of the multiplicity is provided by the Kharzeev-Levin-Nardi (KLN) $k_\perp$-factorization approach [17]. The KLN *ansatz* for the unintegrated gluon distribution functions (uGDFs) of the colliding nuclei incorporates perturbative gluon saturation at high energies and determines the $p_\perp$-integrated multiplicity from weak-coupling QCD without additional models for soft particle production.

Specifically, the number of gluons that are released from the wavefunctions of the colliding nuclei is given by

$$\frac{dN_g}{d^2r_\perp dy} = \mathcal{N}\frac{N_c}{N_c^2-1}\int\frac{d^2p_\perp}{p_\perp^2}\int^{p_\perp} d^2k_\perp\,\alpha_s(k_\perp) \times\phi_A(x_1,(\boldsymbol{p}_\perp+\boldsymbol{k}_\perp)^2/4;\boldsymbol{r}_\perp) \times\phi_B(x_2,(\boldsymbol{p}_\perp-\boldsymbol{k}_\perp)^2/4;\boldsymbol{r}_\perp), \tag{21}$$

where $N_c = 3$ is the number of colors, and $p_\perp$, y are the transverse momentum and the rapidity of the produced gluons, respectively. $x_{1,2} = p_\perp \exp(\pm y)/\sqrt{s_{NN}}$ denote the light-cone momentum fractions of the colliding gluon ladders, and $\sqrt{s_{NN}} = 200$ GeV is the collision energy.

The normalization factor $\mathcal{N}$ can be fixed from peripheral collisions, where final-state interactions should be suppressed. (Ideally, the normalization could be fixed from $p+p$ collisions; however, this is possible only at sufficiently high energies, when the proton saturation scale is at least a few times Λ_{QCD}.) $\mathcal{N}$ also absorbs next-to-leading order (NLO) corrections; when we compare to measured multiplicities of charged hadrons, it includes as well a factor for the average charged hadron multiplicity per gluon, and a Jacobian for the conversion from rapidity to pseudorapidity.

The uGDFs are written as [17,37,38]

$$\phi\left(x,k_\perp^2;\mathbf{r}_\perp\right) = \frac{1}{\alpha_s\left(Q_s^2\right)}\frac{Q_s^2}{\max\left(Q_s^2,k_\perp^2\right)}P(\boldsymbol{r}_\perp)(1-x)^4. \tag{22}$$

$P(\boldsymbol{r}_\perp)$ denotes the probability of finding at least one nucleon at $\boldsymbol{r}_\perp$ [37,38]. This factor arises because configurations without a nucleon at $\boldsymbol{r}_\perp$ do not contribute to particle production. Note that the perturbative $\sim 1/k_\perp^2$ growth of the gluon density toward small transverse momentum saturates at $k_\perp = Q_s$. Therefore, the $p_\perp$-integrated gluon multiplicity obtained from Eq. (21) is finite.

We should emphasize that the *ansatz* (22) is too simple for an accurate description of high-$p_\perp$ particle production. For example, it does not incorporate the so-called "extended geometric scaling" regime above Q_s, which plays an important role in our understanding of the evolution of high-$p_\perp$ spectra from mid- to forward rapidity in d+Au collisions [39]. However, high-$p_\perp$ particles contribute little to the total multiplicity, and more sophisticated models for the uGDF do

not significantly change the centrality dependence of dN/dy [37].

$Q_s(x, \boldsymbol{r}_\perp)$ denotes the saturation momentum at a given momentum fraction x and transverse coordinate $\boldsymbol{r}_\perp$. It is parametrized as [37,38]

$$Q_s^2(x, \boldsymbol{r}_\perp) = 2\,\mathrm{GeV}^2 \left(\frac{T(\boldsymbol{r}_\perp)/P(\boldsymbol{r}_\perp)}{1.53}\right)\left(\frac{0.01}{x}\right)^{\lambda}. \qquad (23)$$

The $\sim 1/x^\lambda$ growth at small x is expected from the BFKL (Balitsky, Fadin, Kuraev, and Lipatov) evolution and has been verified both in deep inelastic scattering at HERA [40] and in high-$p_\perp$ particle production from d+Au collisions at RHIC [39]; the growth speed is approximately $\lambda \simeq 0.28$. Note that the saturation momentum, as defined in Eq. (23), is "universal" in that it does not depend on the thickness of the collision partner at $\boldsymbol{r}_\perp$ [41].

The centrality dependence of Q_s is determined by the thickness function $T(\boldsymbol{r}_\perp)$, which is simply the density distribution of a nucleus, integrated over the longitudinal coordinate z. Note that the standard Woods-Saxon density distribution is averaged over *all* nucleon configurations, including those without any nucleon at $\boldsymbol{r}_\perp$. For this reason, a factor of $1/P(\boldsymbol{r}_\perp)$ arises in Q_s^2 [37,38]. It prevents Q_s from dropping to arbitrarily small values at the surface of a nucleus (since at least one nucleon must be present at $\boldsymbol{r}_\perp$ or else no gluon is produced at that point). The fact that Q_s is bound from below prevents infrared sensitive contributions from the surface of the nucleus and also makes the uGDF (22) less dependent on "freezing" of the one-loop running coupling.

Figure 1 shows the centrality dependence of the multiplicity, as obtained from Eq. (21) via an integration over the transverse plane. It was noted in Ref. [37] that the multiplicity in the most central collisions is significantly closer to the data than the original KLN prediction [17] if the integration over $\boldsymbol{r}_\perp$ is performed explicitly, rather than employing a mean-field-like approximation, $Q_s^2(\boldsymbol{r}_\perp) \to \langle Q_s^2\rangle(b)$. An even better description of the data can be obtained when event-by-event fluctuations of the positions of the nucleons are taken into account [38]; they lead to a slightly steeper centrality dependence of the multiplicity per participant for very peripheral collisions or small nuclei. However, we focus here on central Au+Au collisions, and hence we neglect this effect.

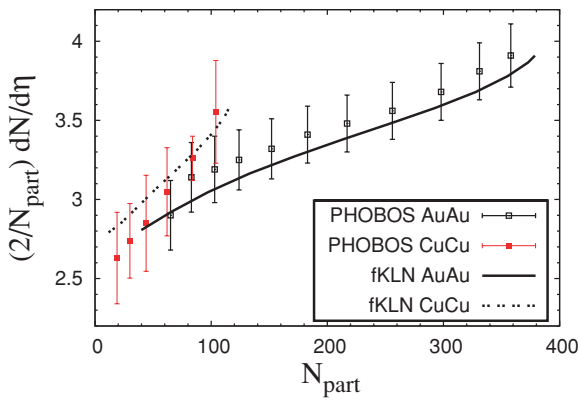

FIG. 1. (Color online) Centrality dependence of the charged particle multiplicity at midrapidity from the $k_\perp$-factorization approach with perturbative gluon saturation at small-x, for Cu+Cu and Au+Au collisions at full RHIC energy, $\sqrt{s_{NN}} = 200$ GeV. PHOBOS data from Ref. [42]; the errors are systematic, not statistical.

It is clear from the figure that the above CGC-$k_\perp$ factorization approach does not leave much room for an additional *centrality-dependent* contribution to the particle multiplicity. (Centrality *independent* gluon multiplication processes have been absorbed into $\mathcal{N}$.) In fact, within the bottom-up thermalization scenario, one does expect, parametrically, that gluon splittings increase the multiplicity by a factor $\sim 1/\alpha^{2/5}$ [43] before the system thermalizes at τ_0 and the hydrodynamic evolution begins. If the scale for running of the coupling is set by Q_s, this would lead to a roughly 20% increase of the multiplicity for the most central Au+Au collisions. However, such a contribution does not seem to be visible in the RHIC data, perhaps because the bottom-up scenario, which considered asymptotic energies, does not apply quantitatively at RHIC energy. It is also conceivable that the model in Eqs. (22) and (23) overpredicts somewhat the growth of the particle multiplicity per participant with centrality.

It is noteworthy that from the most peripheral Cu+Cu to the most central Au+Au bin, $(dN/d\eta)/N_{\mathrm{part}}$ grows by only $\simeq$50% while $N_{\mathrm{part}}^{1/3}$ increases by a factor of 2.6. Clearly, any particle production model that includes a substantial contribution from perturbative QCD processes will cover most of the growth. This implies that rather little entropy production appears to occur after the initial radiation field decoheres. If so, this allows us to correlate the thermalization time τ_0 and the viscosity to entropy density ratio η/s. We shall assume that about 10% entropy production may be allowed for central Au+Au collisions.

The density of gluons at $\tau_s = 1/Q_s$ is given by $dN/d^2r_\perp\, dy$ from Eq. (21), divided by τ_s. For a central collision of Au nuclei at full RHIC energy, the average $Q_s \simeq 1.4$ GeV at midrapidity; hence $\tau_s \simeq 0.14$ fm/c. The parton density at this time is approximately $\simeq$40 fm^{-3}. If their number is effectively conserved[4] until thermalization at τ_0, then

$$n(\tau_0) = \frac{\tau_s}{\tau_0}\, n(\tau_s). \qquad (24)$$

The initial energy density $e(\tau_0)$ can now be obtained from the density via standard thermodynamic relations. We assume that the energy density corresponds to 16 gluons and 3 massless quark flavors in chemical equilibrium, that is,

$$e(T) = \frac{47.5}{30}\pi^2 T^4, \quad n(T) = \frac{43\zeta(3)}{\pi^2}T^3. \qquad (25)$$

Figure 2 shows the parton number and energy densities at τ_0.

[4]We repeat that *centrality-independent* gluon multiplication processes and the contribution from quarks are already accounted for via the normalization factor $\mathcal{N}$.

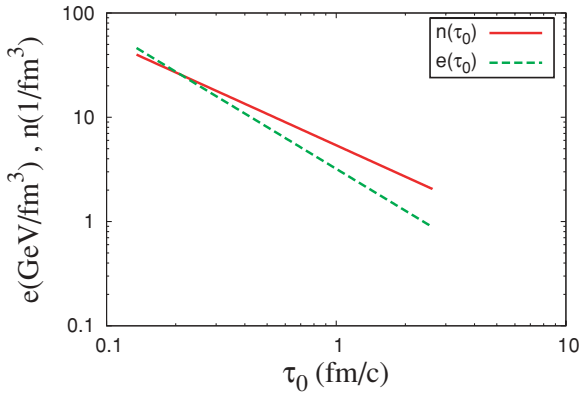

FIG. 2. (Color online) Parton number and energy densities (averaged over the transverse plane) for $b = 0$ Au+Au collisions at $\sqrt{s_{NN}} = 200$ GeV as functions of the thermalization time τ_0.

IV. RESULTS

A. Evolution of entropy and Reynolds number

We begin by illustrating entropy production due to dissipative effects. Given an initial time τ_0 for the hydrodynamic evolution, we determine $\Delta S = dS_{\rm fin}/dy - dS_{\rm ini}/dy$ for $\tau > \tau_0$. This quantity increases rather rapidly at first, since the expansion rate $H \equiv \partial_\mu u^\mu = 1/\tau$ is biggest at small τ. We chose $\tau_{\rm fin} = 5$ fm/c to be on the order of the radius of the collision zone and fix the final value for $\Delta S/S_{\rm ini}$ to equal 10%. Having fixed the initial and final entropy as well as the initial time, we can then determine η/s.

The result of the calculation is shown in Fig. 3. As expected, if the hydrodynamic expansion starts later (larger τ_0), then less entropy is produced for a given value of η/s; conversely, for fixed entropy increase, larger values of η/s are possible. This is due to two reasons: the total time interval for the one-dimensional hydrodynamic expansion as well as the entropy production rate decrease. In fact, the figure shows that for very small initial time, the $\Delta S/S_{\rm ini} = 10\%$ bound cannot be satisfied with $\eta/s \geqslant 1/(4\pi) \simeq 0.08$.

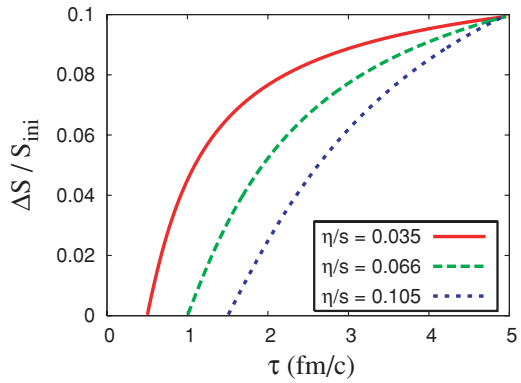

FIG. 3. (Color online) Entropy production within second-order dissipative hydrodynamics as a function of (proper) time; the initial value of the stress is $\Phi(\tau_0) = \Phi_0^*$, cf. Eq. (15). Curves for three different initial times, $\tau_0 = 0.5$, 1, and 1.5 fm/c are shown; for each curve, η/s is chosen such that $\Delta S/S_{\rm ini} = 10\%$ at $\tau_{\rm fin} = 5$ fm/c.

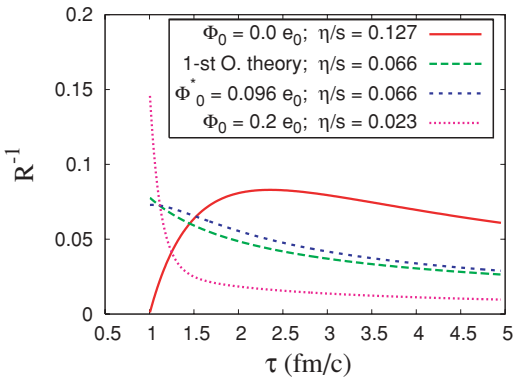

FIG. 4. (Color online) Time evolution of the inverse Reynolds number (using the Boltzmann relaxation time) for different initial values of the viscous stress Φ_0 and of the viscosity to entropy density ratio η/s. The initial time is $\tau_0 = 1$ fm/c for all curves. The short-dashed (blue) line corresponds to the initial condition $\dot{R}(\tau_0) = 0$, cf. Eq. (15). The long-dashed (green) line corresponds to the first-order theory.

In Fig. 4, we show the behavior of the inverse Reynolds number for different initial values of stress. Again, for each curve, η/s is fixed such that $\Delta S/S_{\rm ini} = 10\%$ at $\tau_{\rm fin} = 5$ fm/c. As already indicated above, if $\Phi_0 < \Phi_0^*$ defined in Eq. (15), the fluid cannot compete with the expansion and departs from equilibrium. On the other hand, if $\Phi_0 > \Phi_0^*$, there is already a rapid approach toward the perfect-fluid limit at τ_0. In either case, the interpretation of τ_0 as the earliest possible starting time for hydrodynamic evolution does not appear to be sensible. The initial condition corresponding to $\dot{R}(\tau_0) = 0$ in turn corresponds to the situation in which the fluid has just reached the ability to approach equilibrium. It is clear from the figure that the evolution is close to that predicted by the first-order theory.

Figure 5 shows the Reynolds number for our *ansatz* (13) for the relaxation time at strong coupling, which essentially follows the behavior given by the first-order theory: after a time $\sim\tau_\pi$ has elapsed, the behavior of R is nearly independent of the initial value of Φ. The initial condition $\Phi_0 = \Phi_0^*$ again leads to the most natural behavior of R without a very rapid initial evolution.

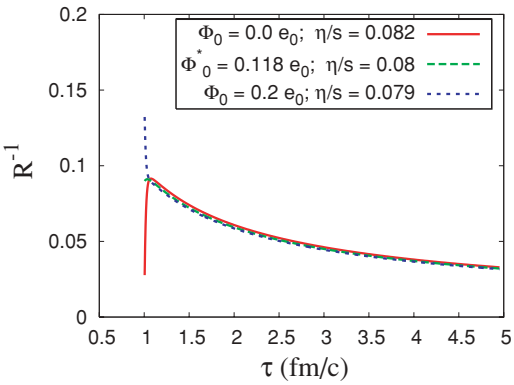

FIG. 5. (Color online) Same as Fig. 4, but for the generalized AdS/CFT relaxation time in Eq. (13).

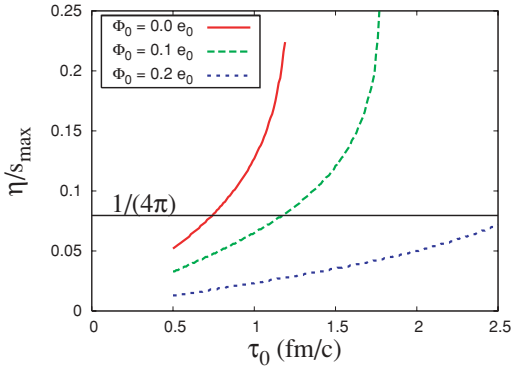

FIG. 6. (Color online) Bound on η/s as a function of τ_0, for $\Delta S/S_{\rm ini} = 10\%$ entropy production, for a Boltzmann gas.

B. η/s versus τ_0

From the previous results, it is evident that fixing the amount of produced entropy, $\Delta S/S_{\rm ini}$, correlates η/s with τ_0. In this section, we show the upper limit of η/s as a function of τ_0.

We begin with the Boltzmann gas with fixed Φ_0 (independent of τ_0) in Fig. 6. One observes that the maximal viscosity depends rather strongly on the initial value of the stress. For any given Φ_0, $(\eta/s)_{\rm max}$ first grows approximately linearly with τ_0. For large initial time, however, the expansion and entropy production rates drop so much that the bound on viscosity eventually disappears. Furthermore, it is interesting to observe that the conjectured lower bound $\eta/s = 1/(4\pi)$ excludes too rapid thermalization: even if the fluid is initially perfectly equilibrated ($\Phi_0 = 0$), a thermalization time well below $\sim$1 fm/c is possible only if either $\eta/s < 1/(4\pi)$ or $\Delta S/S_{\rm ini} > 10\%$. With 10% correction to perfect fluidity at τ_0, shown by the long-dashed (green) line in Fig. 6, the minimal τ_0 compatible with both $\eta/s \geqslant 1/(4\pi)$ and $\Delta S/S_{\rm ini} = 10\%$ is about 1.2 fm/c. If $\eta/s \simeq 0.1$–0.2, as deduced from the centrality dependence of elliptic flow at RHIC [6], then $\tau_0 \simeq 1.5$ fm/c.

In Fig. 7, we perform a similar analysis for our *ansatz* (13) for the strong-coupling case. Because of the much smaller relaxation time of the viscous stress, we observe that the viscosity bound is now rather insensitive to the magnitude of the initial correction to equilibrium. We obtain a lower bound on the thermalization time of $\tau_0 \simeq 1$ fm/c for the minimal viscosity, increasing to about 1.2–2.2 fm/c if $\eta/s \simeq 0.1$–0.2.

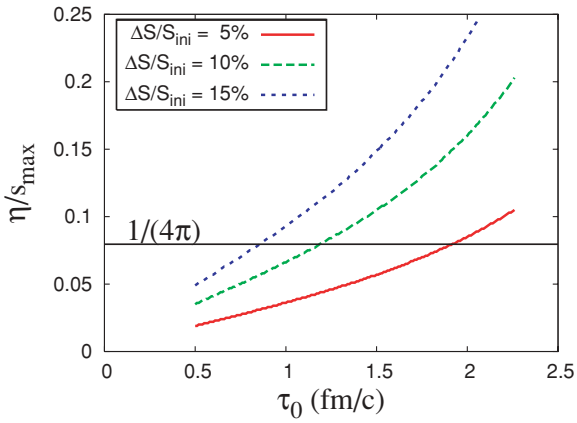

FIG. 8. (Color online) Same as Fig. 6, but for $\Phi_0 = \Phi_0^*$ and different bounds on entropy production.

In Fig. 8, we return to the Boltzmann gas with initial value for the stress as given in Eq. (15), corresponding to $\dot{R}(\tau_0) = 0$. Comparing it to Fig. 6, we observe that the viscosity bound is affected mostly for large τ_0: with this initial condition, a high viscosity $\eta/s \sim 1$ is excluded even if the initial time is as large as 2 fm/c. The reason why the upper bound on the viscosity does not disappear at large τ_0 for this initial stress is that Φ_0^*/e_0 grows with η/s, cf. Eq. (15). A lot of entropy would then be produced, even for large τ_0.

Figure 8 also gives an impression of the sensitivity to the entropy production bound. For $\eta/s = 0.15$, for example, τ_0 decreases from $\simeq$1.8 fm/c, if the entropy is allowed to increase by 10%, to $\simeq$1.5 fm/c if the bound is relaxed to $\Delta S/S_{\rm ini} = 15\%$.

We performed similar calculations for the strong-coupling limit as shown in Fig. 9. The curves are rather close to those for a Boltzmann gas from Fig. 8, which is expected. With this initial condition, i.e., $\Phi_0 = \Phi_0^*$, the hydrodynamic evolution is close to the first-order theory for both cases.

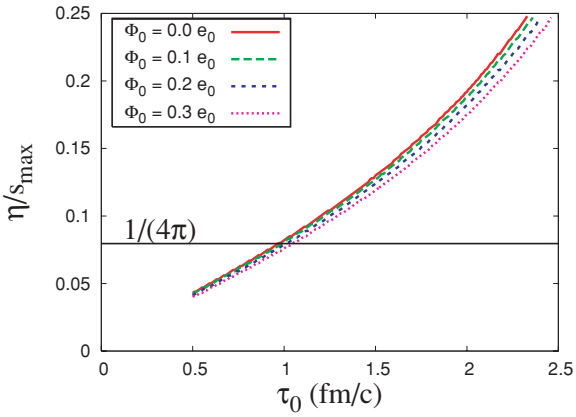

FIG. 7. (Color online) Same as Fig. 6, but for strong coupling, τ_π from Eq. (13).

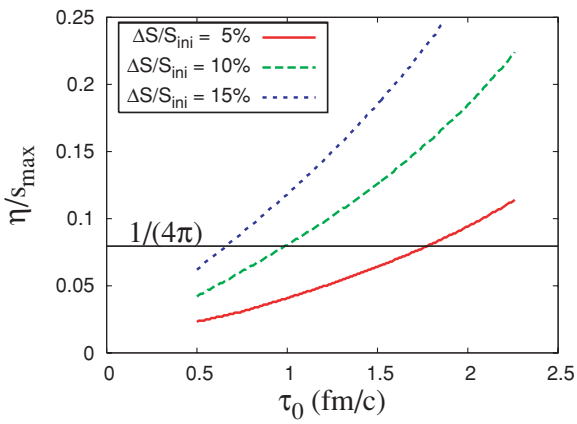

FIG. 9. (Color online) Same as Fig. 8, but for the strong-coupling limit, i.e., for τ_π from Eq. (13).

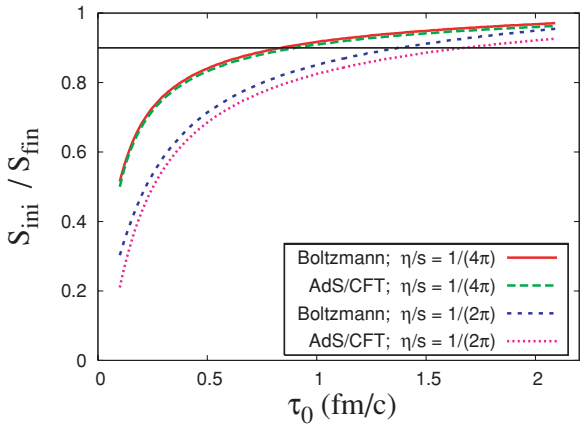

FIG. 10. (Color online) Initial over final entropy as a function of τ_0 for two different values of η/s, and two different relaxation times corresponding to weak and strong coupling.

Entropy production is sensitive only to τ_0 and η/s but is nearly independent of the stress relaxation time τ_π.

Figure 10 shows the ratio of the final to the initial entropy as a function of τ_0 for two different values of η/s, and the two different relaxation times discussed above in Eqs. (12) and (13). Here, $S_{\rm fin}$ has been fixed to the value appropriate for central Au+Au collisions, while $S_{\rm ini}$ is varied accordingly. For example, for $\tau_0 = 0.6$ fm/c and $\eta/s = 1/(2\pi)$, almost 30% entropy production occurs. This would account for the entire growth of $(dN/d\eta)/N_{\rm part}$ from $N_{\rm part} \simeq 60$ to $N_{\rm part} \simeq 360$ observed in Fig. 1. That is, for these parameters, the initial parton multiplicity per participant would have to be completely independent of centrality. For the same viscosity, $\tau_0 = 0.3$ fm/c would imply that nearly half of the final-state entropy was produced during the hydrodynamic stage, i.e., that the initial multiplicity per participant should actually *decrease* with centrality. Such a scenario appears unlikely to us. Note that even for $\tau_0 = 0.3$ fm/c and $\eta/s = 1/(4\pi)$, with $T = 400$ MeV one finds that $\Gamma_s(\tau_0)/\tau_0 \simeq 0.17$ is quite small. Romatschke obtained similar numbers for the initial to final entropy ratio, albeit only for $\tau_0 = 1$ fm/c, in a computation that included cylindrically symmetric transverse expansion [28].

V. SUMMARY, DISCUSSION, AND OUTLOOK

In this paper, we have analyzed entropy production due to nonzero shear viscosity in central Au+Au collisions at RHIC. We point out that a good knowledge of the *initial conditions*, and of the final state, of course, can provide useful constraints for hydrodynamics of high-energy collisions, specifically on transport coefficients, on the equation of state (not discussed here, cf. Ref. [6]), on the initial/thermalization time and so on.

Our main results are as follows. Assuming that hydrodynamics applies at $\tau > \Gamma_s$, then due to the rather restrictive bound on entropy production, it follows that the shear viscosity to entropy density ratio of the QCD matter produced at central rapidity should be small, at most a few times the lower bound $\eta/s = 1/(4\pi)$ conjectured from the AdS/CFT correspondence at infinite coupling. This represents a consistency check with similar numbers ($\eta/s \lesssim 0.2$) extracted from azimuthally asymmetric elliptic flow [4–7]. We have neglected several other possible sources of entropy production, such as bulk viscosity near the transition region [35] or hadronic corona effects [23]; such additional contributions might tighten the constraints even further.

Furthermore, the entropy production bound correlates the maximal allowed viscosity to the initial time τ_0 for hydrodynamic evolution. This is because the expansion rate is equal to the inverse of the expansion time, which makes entropy production from viscous effects rather sensitive to the value of τ_0. We have found that for $\Delta S/S_{\rm ini} \simeq 10\%$, the initial time for hydrodynamics should be around 1 fm/c, possibly a little larger. Significantly smaller thermalization times would either require $\eta/s < 0.15$–0.2 [or even smaller than $1/(4\pi)$]. Alternatively, they would require a particle production mechanism that yields significantly lower initial multiplicities than the KLN-CGC approach. Given the very good description of the centrality dependence of the multiplicity, however, it appears reasonable to us to assume that this approach provides an adequate initial condition in that the initial parton multiplicity per participant increases with centrality.

A significant problem with viscous hydrodynamics, in particular with the Israel-Stewart second-order approach, is that the number of initial parameters increases. Even within the most simple framework followed here (1+1D Bjorken expansion combined with neglect of conserved currents, bulk viscosity, and heat flow), a unique solution requires us to specify, in addition to the ideal-fluid parameters, the shear viscosity and the initial value for the stress. The latter, in particular, is not a general property of near-equilibrium QCD but depends on the parton liberation and thermalization process. We have, however, introduced a physically motivated initial condition for the stress: if τ_0 is defined as the earliest possible initial time for hydrodynamics, it is plausible that the initial Reynolds number should be stationary, $\dot{R}(\tau_0) = 0$. Otherwise, the fluid either still departs from equilibrium [$\dot{R}(\tau_0) < 0$] or is already approaching it [$\dot{R}(\tau_0) > 0$].

For small relaxation times of the stress, the condition that $\dot{R}(\tau_0) = 0$ implies that its initial value is already close to that given by the first-order theory of Eckart, Landau, and Lifshitz (the relativistic generalization of Navier-Stokes hydrodynamics). We therefore expect that in general the two approaches will provide rather similar results for heavy-ion collisions. One should keep in mind, however, that in the second-order theory, the entropy current includes a term quadratic in the stress, which is of course absent from the first-order theory and which slightly reduces entropy production.

Perhaps most importantly, with $\dot{R}(\tau_0) = 0$, the hydrodynamic evolution is largely independent of the stress relaxation time τ_π, and therefore similar for both a Boltzmann gas at weak coupling (with low viscosity, however) and a strongly coupled plasma. The latter relaxes very rapidly to the first-order theory, regardless of the initial condition. The former, on the other hand, is forced by the initial condition to start close to relativistic Navier-Stokes, and the relaxation time is still sufficiently small to prevent a significant departure from the first-order theory.

The initial condition $\dot{R}(\tau_0) = 0$ also guarantees that $R(\tau) \gg 1$ for all $\tau \geqslant \tau_0$, as long as the initial time is not extremely short ($\tau_0 T_0 \gg \eta/s$). The effective enthalpy $(1 - 1/R)(e + p)$ is therefore always positive. On the other hand, our numerical results indicate that the Reynolds number does not exceed ~100 during the QGP phase. This is well below the regime where Navier-Stokes turbulence occurs in incompressible, nonrelativistic fluids ($R \gtrsim 1000$). Indeed, turbulence during the hydrodynamic stage would probably cause large fluctuations of the elliptic flow v_2 [44], which are not seen [45].

A quantitative interpretation of hydrodynamic flow effects in heavy-ion collisions at RHIC and the CERN Large Hadron Collider (LHC) will of course require 2+1D and 3+1D solutions [7,24–29]. The results obtained here should prove useful for constraining the initial conditions (in particular τ_0 and Φ_0) for such large-scale numerical efforts. In particular, as we pointed out here, the entropy production bound correlates τ_0 with η/s. In turn, we expect that elliptic flow will provide an *anticorrelation,* since later times and larger shear viscosity should both reduce its magnitude. The intersection of those curves could then provide an estimate of the initial time for hydrodynamics at RHIC.

ACKNOWLEDGMENTS

The authors would like to thank L. P. Csernai, H. J. Drescher, M. Gyulassy, D. H. Rischke, D. Schiff, and H. Stöcker for useful discussions. E. M. gratefully acknowledges support by the Alexander von Humboldt foundation.

[1] The experimental results of the four collaborations at RHIC are summarized and interpreted in I. Arsene *et al.* (BRAHMS Collaboration), Nucl. Phys. **A757**, 1 (2005); B. B. Back *et al.*, *ibid.* **A757**, 28 (2005); J. Adams *et al.* (STAR Collaboration), *ibid.* **A757**, 102 (2005); K. Adcox *et al.* (PHENIX Collaboration), *ibid.* **A757**, 184 (2005).
[2] For a recent review, see, for example, P. Huovinen and P. V. Ruuskanen, Annu. Rev. Nucl. Part. Sci. **56**, 163 (2006).
[3] See, e.g., D. H. Rischke, S. Bernard, and J. A. Maruhn, Nucl. Phys. **A595**, 346 (1995).
[4] D. Teaney, Phys. Rev. C **68**, 034913 (2003).
[5] R. A. Lacey *et al.*, Phys. Rev. Lett. **98**, 092301 (2007).
[6] H. J. Drescher, A. Dumitru, C. Gombeaud, and J. Y. Ollitrault, arXiv:0704.3553.
[7] P. Romatschke and U. Romatschke, arXiv:0706.1522v1.
[8] L. P. Csernai, J. I. Kapusta, and L. D. McLerran, Phys. Rev. Lett. **97**, 152303 (2006).
[9] H. B. Meyer, arXiv:0704.1801.
[10] P. K. Kovtun, D. T. Son, and A. O. Starinets, Phys. Rev. Lett. **94**, 111601 (2005).
[11] S. Gavin and M. Abdel-Aziz, Phys. Rev. Lett. **97**, 162302 (2006).
[12] A. Adare *et al.* (PHENIX Collaboration), Phys. Rev. Lett. **98**, 172301 (2007).
[13] A. Hosoya and K. Kajantie, Nucl. Phys. **B250**, 666 (1985); P. Danielewicz and M. Gyulassy, Phys. Rev. D **31**, 53 (1985); H. Heiselberg and X. N. Wang, Phys. Rev. C **53**, 1892 (1996).
[14] A. Muronga, Phys. Rev. Lett. **88**, 062302 (2002); **89**, 159901(E) (2002); Phys. Rev. C **69**, 034903 (2004).
[15] W. Israel, Ann. Phys. (NY) **100**, 310 (1976); J. M. Stewart, Proc. R. Soc. London Ser. A **357**, 57 (1977); W. Israel and J. M. Stewart, Ann. Phys. (NY) **118**, 341 (1979).
[16] J. D. Bjorken, Phys. Rev. D **27**, 140 (1983).
[17] D. Kharzeev and M. Nardi, Phys. Lett. **B507**, 121 (2001); D. Kharzeev, E. Levin, and M. Nardi, Nucl. Phys. **A730**, 448 (2004); **743**, 329(E) (2004); **A747**, 609 (2005).
[18] X. N. Wang and M. Gyulassy, Phys. Rev. Lett. **86**, 3496 (2001).
[19] A. Krasnitz, Y. Nara, and R. Venugopalan, Nucl. Phys. **A717**, 268 (2003).
[20] M. P. Heller and R. A. Janik, Phys. Rev. D **76**, 025027 (2007).
[21] M. Lublinsky and E. Shuryak, Phys. Rev. C **76**, 021901(R) (2007).
[22] Y. V. Kovchegov and A. Taliotis, arXiv:0705.1234.
[23] T. Hirano and M. Gyulassy, Nucl. Phys. **A769**, 71 (2006).
[24] U. W. Heinz, H. Song, and A. K. Chaudhuri, Phys. Rev. C **73**, 034904 (2006).
[25] A. Muronga and D. H. Rischke, arXiv:nucl-th/0407114.
[26] R. Baier, P. Romatschke, and U. A. Wiedemann, Phys. Rev. C **73**, 064903 (2006).
[27] R. Baier and P. Romatschke, arXiv:nucl-th/0610108.
[28] P. Romatschke, arXiv:nucl-th/0701032.
[29] A. Muronga, Phys. Rev. C **76**, 014909 (2007).
[30] R. S. Bhalerao and S. Gupta, arXiv:0706.3428.
[31] C. Eckart, Phys. Rev. **58**, 919 (1940).
[32] L. D. Landau and E. M. Lifshitz, *Fluid Dynamics*, Second Ed. (Butterworth-Heinemann, London, 1987).
[33] T. Koide, Phys. Rev. E **75**, 060103(R) (2007).
[34] P. Arnold, C. Dogan, and G. D. Moore, Phys. Rev. D **74**, 085021 (2006).
[35] See, e.g., the paper by P. Danielewicz and M. Gyulassy quoted in Ref. [13]; also see, L. P. Csernai and J. I. Kapusta, Phys. Rev. Lett. **69**, 737 (1992); for more recent approaches, K. Paech and S. Pratt, Phys. Rev. C **74**, 014901 (2006); D. Kharzeev and K. Tuchin, arXiv:0705.4280.
[36] G. Baym, Nucl. Phys. **A418**, 525C (1984).
[37] A. Adil, H. J. Drescher, A. Dumitru, A. Hayashigaki, and Y. Nara, Phys. Rev. C **74**, 044905 (2006).
[38] H. J. Drescher and Y. Nara, Phys. Rev. C **75**, 034905 (2007).
[39] A. Dumitru, A. Hayashigaki, and J. Jalilian-Marian, Nucl. Phys. **A765**, 464 (2006); **A770**, 57 (2006).
[40] K. Golec-Biernat and M. Wusthoff, Phys. Rev. D **59**, 014017 (1998); **60**, 114023 (1999).
[41] T. Lappi and R. Venugopalan, Phys. Rev. C **74**, 054905 (2006).
[42] B. B. Back *et al.* (PHOBOS Collaboration), Phys. Rev. C **65**, 061901 (2002); G. Roland (PHOBOS Collaboration), Nucl. Phys. **A774**, 113 (2006).
[43] R. Baier, A. H. Mueller, D. Schiff, and D. T. Son, Phys. Lett. **B539**, 46 (2002).
[44] S. Vogel, G. Torrieri, and M. Bleicher, arXiv:nucl-th/0703031.
[45] P. Sorensen (STAR Collaboration), arXiv:nucl-ex/0612021; B. Alver *et al.* (PHOBOS Collaboration), arXiv:nucl-ex/0702036, Phys. Rev. Lett. (to be published).